PAPER *Special Section on Microwave and Millimeter-Wave Technologies*

Efficiency Enhancement of a Single-Diode Rectenna Using Harmonic Control of the Antenna Impedance

Katsumi KAWAI[†a)], ***Student Member***, **Naoki SHINOHARA**[†], ***Senior Member***, ***and*** **Tomohiko MITANI**[†], ***Member***

SUMMARY This study introduces a novel single-diode rectenna, enhancing the rf–dc conversion efficiency using harmonic control of the antenna impedance. We employ source-pull simulations encompassing the fundamental frequency and the harmonics to achieve a highly efficient rectenna. The results of the source-pull simulations delineate the source-impedance ranges required for enhanced efficiency at each harmonic. Based on the source-pull simulation results, we designed two inverted-F antenna with input impedances within and without these identified source impedance ranges. Experimental results show that the proposed rectenna has a maximum rf–dc conversion efficiency of 75.9% at the fundamental frequency of 920 MHz, an input power of 10.8 dBm, and a load resistance of 1 kΩ, which is higher than that of the comparative rectenna without harmonic control of the antenna impedance. This study demonstrates that the proposed rectenna achieves high efficiency through the direct connection of the antenna and the single diode, along with harmonic control of the antenna impedance.

key words: *rectenna, harmonic control, source-pull simulation, single-series, wireless power transfer (WPT)*

1. Introduction

A circuit comprising a receiving antenna and a rectifier circuit—termed a "rectenna" by William C. Brown—is a fundamental component in far-field wireless power transfer. Figure 1 illustrates the distinctions between the single-shunt and single-series rectennas circuit diagrams. Brown introduced a single-shunt rectenna with a half-wave dipole antenna and a parallel-connected rectifying diode, which we classify as a type I rectenna in Fig. 1 [1]. His single-shunt rectifier circuit utilizes the properties of a distributed circuit to control the harmonics generated by the diode. Notably, the dc-pass filter, which consists of a quarter-wavelength line and a smoothing capacitor, acts as an open circuit for the odd harmonics and a short circuit for the even harmonics generated by the diode. This harmonic control enables full-wave rectification using a single diode [2]. Brown achieved an rf–dc conversion efficiency of 90% with a 2.45 GHz-band single-shunt rectenna [1].

Several researchers have focused on the similarities between harmonic control of the dc-pass filter of a single-shunt rectenna and it of a Class-F load of a high-frequency amplifier [3]–[7]. Several studies have documented using single-shunt rectifier circuits that employ a Class-F load. The capacitor in the dc-pass filter fails to provide adequate short-circuit terminations at the higher harmonics, however, due to the frequency characteristics of the capacitor. In the Class-F load configuration shown as type I in Fig. 1, the capacitor is replaced with parallel-connected open stubs that constitute quarter-wavelength resonators for the fundamental frequency and harmonics. These open stubs fine-tune the short-circuit terminations at the fundamental frequency and each harmonic, resulting in a more efficient rectifier circuit compared to one that uses a capacitor. Previous studies have reported single-shunt rectifier circuits using a Class-F load, achieving an efficiency of 90% at the 2.45 GHz band [3] and 91% at the 920 MHz band [4]. Therefore, harmonic control is essential for achieving full-wave rectification and high efficiency with a single diode, as demonstrated in a single-shunt rectenna.

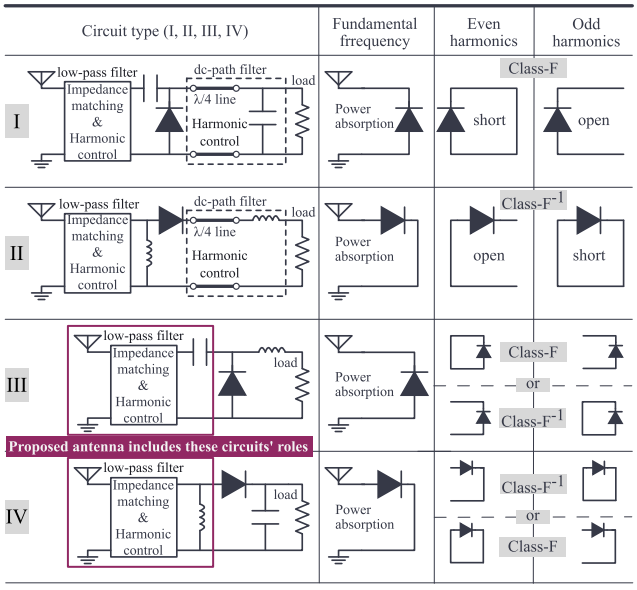

Fig. 1 Comparison of the differences between single-shunt and single-series rectennas and the configuration of the proposed single-series rectenna.

Diode efficiency limits the maximum rf–dc conversion efficiency of a rectenna [8]. It is, therefore, crucial not only to determine the maximum efficiency of the diode under operational conditions but also to minimize circuit losses in peripheral components. Thus, it is essential to consider designing a rectenna with a simple configuration. In the standard design of a single-diode rectenna, as shown in Fig. 1, either the dc pass filter, the low pass filter, or both are responsible for harmonic control. Concurrently, the low pass filter

Manuscript received October 6, 2023.
Manuscript revised February 9, 2024.
Manuscript publicized April 9, 2024.

[†]Research Institute for Sustainable Humanosphere, Kyoto University, Uji-shi, 611–0011 Japan.
a) E-mail: kawai.katsumi.38m@st.kyoto-u.ac.jp

DOI: 10.1587/transele.2024MMP0002

also facilitates impedance matching between the receiving antenna and the rectifier circuit. The operating conditions of the rectifying diode vary with the input power and the load resistance. Typically, the low-pass filter is optimized for a specific operating condition of the diode. Therefore, it is crucial to consolidate harmonic control and impedance matching into a single component to minimize circuit losses. A previous study [9] introduced a highly efficient rectenna featuring a direct connection between a half-wave dipole antenna and a full-bridge rectifier circuit without the low pass filter. Harmonic control was achieved by using short stubs connected to the antenna, which resulted in the impressive rf–dc conversion efficiency of 92.8% [9]. However, the full-bridge rectenna features a cross-connection at the dc pass filter, which complicates the configuration in the case of a single-layered rectenna. Therefore, to achieve higher rf–dc conversion efficiency, a single-diode rectenna is needed that eliminates the need for cross-connections at the dc pass filter and simplifies the configuration by avoiding additional circuits.

This study introduces a novel single-diode rectenna, shown as type IV in Fig. 1, which enhances the rf–dc conversion efficiency by using harmonic control of the receiving antenna impedance. This study focuses on developing a single-series rectenna equipped with an antenna capable of controlling the harmonics. Namely, the roles of the low-pass filter and an inductor for the dc short circuit are integrated into the receiving antenna. This configuration can minimize losses in additional circuits and improve the rf–dc conversion efficiency. Notable distinctions between our proposed rectenna and a single-shunt rectenna that utilizes a Class-F load include our ability to simplify the dc-pass filter by implementing harmonic control at the antenna. Additionally, our rectenna differs from the full-bridge rectenna presented in [9] in that it achieves full-wave rectification using only a single diode. We incorporate source-pull simulations in designing our rectenna. Source/load-pull techniques are commonly used in high-frequency amplifier design [10]–[12]. They also apply to rectenna design, as it involves non-linear elements similar to those in high-frequency amplifiers. Although previous research has covered rectenna design extensively using load-pull methods [13]–[17], designs employing source-pull techniques are less common. Moreover, previous investigations into the use of source-pull methods for rectenna design have focused on the fundamental frequency alone [18]–[22]. A previous study [23] did utilize multi-harmonic active source-pull in the MHz band for rectifier design. However, the rectifier in [23] is transistor-based, not diode-based. Consequently, this study employs source-pull simulations that encompass the fundamental frequency and the harmonics in designing a diode-based single-series rectenna.

This paper is structured as follows: Sect. 1 discusses previous rectenna studies and outlines the objectives of this study. Section 2 highlights distinctions between single-shunt and single-series rectennas, emphasizing the advantages of single-series rectennas. Using ideal-circuit simulations, we have also demonstrated that a single-series rectenna can achieve an ideal 100% efficiency when the antenna controls the harmonics. In Sect. 3, we design a 920 MHz-band proposed single-series rectenna with harmonic control of the antenna impedance using source-pull simulations with harmonics. Furthermore, we have designed a comparative rectenna without harmonic control of the antenna impedance to validate the effectiveness of harmonic control of the antenna impedance in enhancing efficiency. Section 4 details the experimental results and compares the performance of the designed rectennas with and without harmonic control of the antenna impedance. The paper concludes in Sect. 5, summarizing our key findings and contributions.

2. Principle of the Proposed Rectenna

2.1 Feature Comparison between the Single-Shunt and the Single-Series Rectenna

Theoretically, a single-shunt rectenna, which utilizes a quarter-wavelength line and a capacitor, can attain 100% rf–dc conversion efficiency. Conversely, the dc-pass filter of the type II single-series rectenna shown in Fig. 1, which employs a quarter-wavelength line and an inductor, creates an open circuit at even harmonics and a short circuit at odd harmonics. Consequently, the ideal rf–dc conversion efficiency of this single-series rectenna reaches 100% due to this harmonic control, enabling the diode to be used for inverted-F (Class-F^{-1}) operation [24], [25]. In contrast, in the case that harmonic control is concentrated in the low-pass filter as shown in type III and IV in Fig. 1, both Class-F and Class-F^{-1} operations become applicable for single-shunt and single-series rectenna configurations.

In a single-shunt rectenna, the dc-pass filter must be an open circuit at the fundamental frequency to ensure that the input power is directed solely to the diode and does not flow to the load. Consequently, if the low-pass filter controls the harmonics in a single-shunt rectenna, the dc-pass filter requires an inductor connected in series, as shown in type III in Fig. 1. In contrast, in a single-series rectenna, the dc-pass filter must be a short circuit at the fundamental frequency to ensure that the input power is directed solely to the diode and does not flow to the load, as shown in type IV in Fig. 1. Therefore, if the low-pass filter controls the harmonics in the single-series rectenna, the dc-pass filter requires a capacitor connected in parallel. Capacitors generally have lower losses than inductors, as indicated by their higher non-loaded quality factor Q. A type III single-shunt rectenna can omit the series-connected capacitor on the rectenna's input side when an open-ended antenna, such as a patch antenna, is utilized. Likewise, a type IV single-series rectenna can omit the parallel-connected inductor on the rectenna's input side when a short-ended antenna, like an inverted-F antenna, is employed. Consequently, a single-series rectenna that relies solely on a capacitor is more likely to reduce circuit losses than a single-shunt rectenna, which requires an inductor. This feature of the single-series rectenna is advantageous

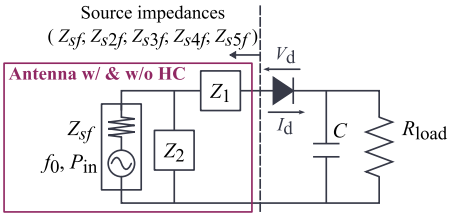

	DC	f_0	$2f_0$	$3f_0$	$4f_0$	$5f_0$
Z_1	0 Ω	0 Ω	Z_{s2f}	Z_{s3f}	Z_{s4f}	Z_{s5f}
Z_2	0 Ω	10^{21} Ω	0 Ω	0 Ω	0 Ω	0 Ω

Fig. 2 Circuit diagram for a comparative analysis of two cases: with and without harmonic control at the antenna. The resistances 0 Ω and 10^{21} Ω represent a short circuit and an open circuit, respectively.

for rectenna design. Based on these advantages, this study focused on and designed the single-series rectenna. Furthermore, this study proposes a new single-series rectenna that integrates the roles of the low-pass filter and shunt inductor in the receiving antenna and performs harmonic control at the receiving antenna.

2.2 Simulation of the Single-Series Rectenna Using Ideal Circuits

The previous study [26] established the theoretical efficiency of a single-series rectifier circuit at 81.1%. However, this study [26] did not incorporate harmonic control. In this subsection, we use circuit simulations that employ ideal components and circuits to show that when the antenna (functioning as the power supply) controls the harmonics, the rf–dc conversion efficiency of the single-series rectenna can reach 100%. Additionally, as part of the ideal circuit simulation, we carried out a comparative analysis of two cases: with and without harmonic control at the antenna (the power supply).

Figure 2 shows the circuit diagram for a simulation using the Advanced Design System (ADS) from Keysight Technologies. We used the harmonic balance method, with the maximum order set to be the fifth harmonic. The fundamental frequency, denoted by f_0, was 920 MHz. The input power was 10.0 dBm, and the load resistance was 1 kΩ. In this simulation, we utilized an ideal diode, represented within the circuit using the following equation:

$$I_\mathrm{d} = \begin{cases} 0 & (V_\mathrm{d} < 0), \\ \frac{V_\mathrm{d}}{R_\mathrm{d}} & (V_\mathrm{d} \geq 0), \end{cases} \tag{1}$$

where I_d represents the current through the diode, V_d represents the voltage, and $R_\mathrm{d} = 0.5\,\mathrm{m\Omega}$ represents the on-resistance of the diode. We used a 1 nF capacitor as an output-smoothing capacitor. The power supply impedance Z_{sf} and impedances Z_1 and Z_2 determined the source impedances at the fundamental frequency and harmonics. We configured the source impedances at each harmonic Z_{snf} using the magnitude M_n and phase D_n of the reflection coefficients S_{snf}, as defined by the following equations:

$$Z_{snf} = Z_0 \frac{1 + S_{snf}}{1 - S_{snf}} \quad (n = 1, 2, \ldots, 5), \tag{2}$$

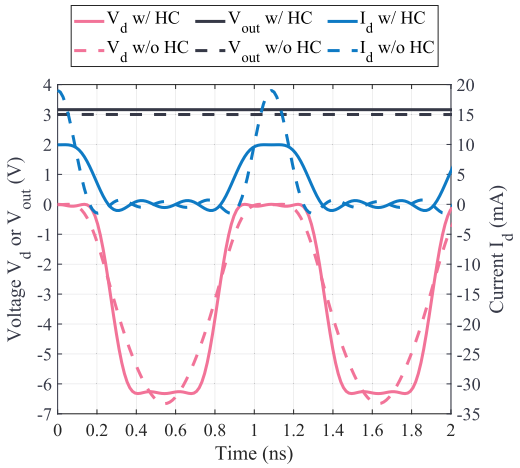

Fig. 3 Voltage (red) and current waveforms (blue) at the diode and the output DC voltage (black) with and without harmonic control (HC) in the ideal circuit simulation.

Table 1 Harmonic power at the diode with or without harmonic control (HC) in the ideal circuit simulation.

Num. of harmonic	w/ HC (mW)	w/o HC (mW)
DC	10.0	9.01
f_0	10.0	10.0
$2f_0$	1.00×10^{-5}	5.91×10^{-1}
$3f_0$	3.90×10^{-4}	3.14×10^{-1}
$4f_0$	1.50×10^{-7}	8.80×10^{-2}
$5f_0$	3.00×10^{-5}	2.74×10^{-5}

$$S_{snf} = M_n \exp\left(\mathrm{j} D_n \frac{\pi}{180^\circ}\right) \quad (n = 1, 2, \ldots, 5), \tag{3}$$

where n represents the harmonic order, and Z_0 represents a reference impedance of 50 Ω. We configured the source impedances to create short circuits at the even harmonics and open circuits at the odd harmonics, enabling Class-F operation of the diode. Equations (2) and (3) indicate that Z_{snf} diverges when $M_n = 1$. Consequently, we cannot use $M_n = 1$ due to simulation errors. We therefore used $M_n = 0.9999$ and $D_n = 0^\circ$ to represent an open circuit, while we represented a short circuit by $M_n = 0.9999$ and $D_n = 180^\circ$. In cases where harmonic control was not employed, we set the source impedances at each harmonic to 50 Ω ($M_n = 0$ and $D_n = 0^\circ$ when $n \neq 1$), but not for the fundamental frequency. We optimized the source impedance at the fundamental frequency on the real number to achieve impedance matching for the rectifier circuit in both cases: with and without harmonic control.

Figure 3 shows the voltage and current waveforms at the diode, as observed in the simulation. Table 1 displays the harmonic power at the diode with or without harmonic control in the simulation, rounded to three significant digits. The simulations yield a 100% rf–dc conversion efficiency when harmonic control is applied and a 90.1% efficiency when it is not. These waveforms exhibit square-wave double voltage and half-wave double current patterns in harmonic control. These waveforms are consistent with Class-F operation theory. The simulations indicate that the rf–dc con-

version efficiency for a single-series rectenna reaches 100% with harmonic control, an increase of 9.9% compared to the case without harmonic control. The rf–dc conversion efficiency of the rectenna is associated with the theoretical efficiency with losses from the diode and circuits.

3. Rectenna Design

3.1 Rectifier Design Using the Source-Pull Simulation with Harmonics

Figure 4 shows a circuit diagram of the source-pull simulation for the single-series rectifier circuit. For the dielectric substrate, we used R5775-K from Panasonic, which has the following specifications: dielectric constant = 3.62, tangential constant = 0.0046, substrate thickness = 0.75 mm, and metal thickness = 18 μm. The line width was 1.62 mm with a reference impedance of 50 Ω. The rectifying diode we employed was SMS7621 from Skyworks. Figure 5 and Table 2 show the equivalent circuit and the SPICE parameters of the diode before and after adjustment, respectively. Here, the SPICE parameters provided in the datasheet are tailored for use in small-signal applications such as detector circuits and mixers. Consequently, when these SPICE parameters are employed for rectenna design, discrepancies arise between simulation outcomes and experimental results, particularly under high power inputs that fall within the diode's tolerance range. To address this, we measured the voltage-current characteristics of the diode, and SPICE parameters except C_{j0}, were adjusted based on these measurements as detailed in Table 2. The parameter C_{j0} was fine-tuned through the empirical evaluation of several rectifier circuits utilizing the same diode, ensuring alignment between simulation and experimental results. We used GJM1552C1H430JB01 from Murata for the capacitor, with a capacitance of 43 pF. the dc-pass filter is a simple circuit consisting of a capacitor connected in parallel. It allows dc power to pass to the load while cutting the fundamental frequency and harmonics. We swept the source impedances during the simulation while keeping the input power and load resistance fixed at 10.0 dBm and 1 kΩ, respectively. We determined these source impedances using Eqs. (2) and (3). We varied each harmonic impedance in steps of 0.01, ranging from 0.01 to 0.99 for the magnitude M_n of the reflection coefficient, and in 1° steps, from 0° to 360°, for the phase D_n of the reflection coefficient. Before conducting the source-pull simulation, we optimized the source impedance at each harmonic to maximize efficiency. Then, we swept the source impedance at each harmonic. The source impedances for orders not involved in the source-pull simulation sweep were fixed to the values obtained from optimization.

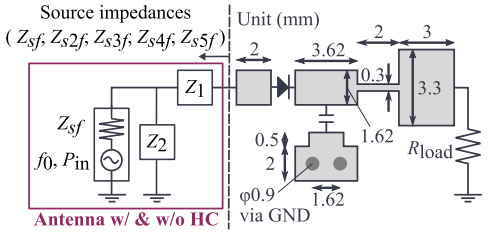

Fig. 4 Circuit diagram of the source-pull simulation for the single-series rectifier circuit.

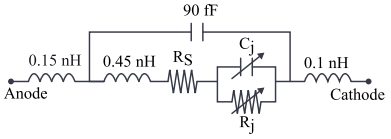

Fig. 5 Equivalent circuit of the diode (SMS7621). The package model is SC-79.

Table 2 SPICE parameters of the diode (SMS7621) before and after adjustment.

	Parameter	Value	Parameter	Value
before adjustment (from datasheet)	I_s	0.4 nA	R_s	12 Ω
	N	1.05	C_{j0}	0.1 pF
	V_j	0.51 V	M	0.35
	B_v	3 V	I_{bv}	10 μA
after adjustment	I_s	2 μA	R_s	9.6 Ω
	N	1.7	C_{j0}	0.15 pF
	V_j	0.3 V	M	0.35
	B_v	8.4 V	I_{bv}	0.8 mA

Figure 6 shows the results of the source-pull simulation, with specific figures for the fundamental frequency (Fig. 6 (a)), the second and fourth harmonics (Fig. 6 (b)), and the third and fifth harmonics (Fig. 6 (c)). In Fig. 6, each plot represents the optimal source impedance at which maximum efficiency is achieved in the simulation. The maximum rf–dc conversion efficiency is 80.4%, resulting in an output dc voltage of 2.84 V. Based on the source-pull simulation results, we established target source impedances for each harmonic within the range where the rf–dc conversion efficiency reaches 79.0% or higher. Figure 6 (a) shows a close-up of the upper right corner of the Smith chart; in this figure, the optimal fundamental source impedance is 153.5 + j271.0 Ω. This result indicates that the fundamental source impedance becomes high when a dc output voltage of several volts is extracted at a low input power of 10.0 dBm. The input impedance of the rectifier circuit is the conjugate value of the source impedance. Consequently, Fig. 6 (a) indicates that the input impedance of the rectifier circuit at the fundamental frequency is capacitive; this occurs because of parasitic capacitances, including the capacitances of both the diode junction and the package. Additionally, Fig. 6 shows that the target range for the fundamental source impedance is narrower than that for other harmonic source impedances. The contour results for the fundamental frequency demonstrate that the rf–dc conversion efficiency changes rapidly with variations in the fundamental source impedance. The source impedances for even harmonics are the second-most critical parameters for the rf–dc conversion efficiency. The second-harmonic source impedance is located in the lower-left corner of the Smith chart, and the fourth-harmonic source impedance is found in the upper right corner, where efficiencies of 79.0% or higher can be achieved. In contrast, the

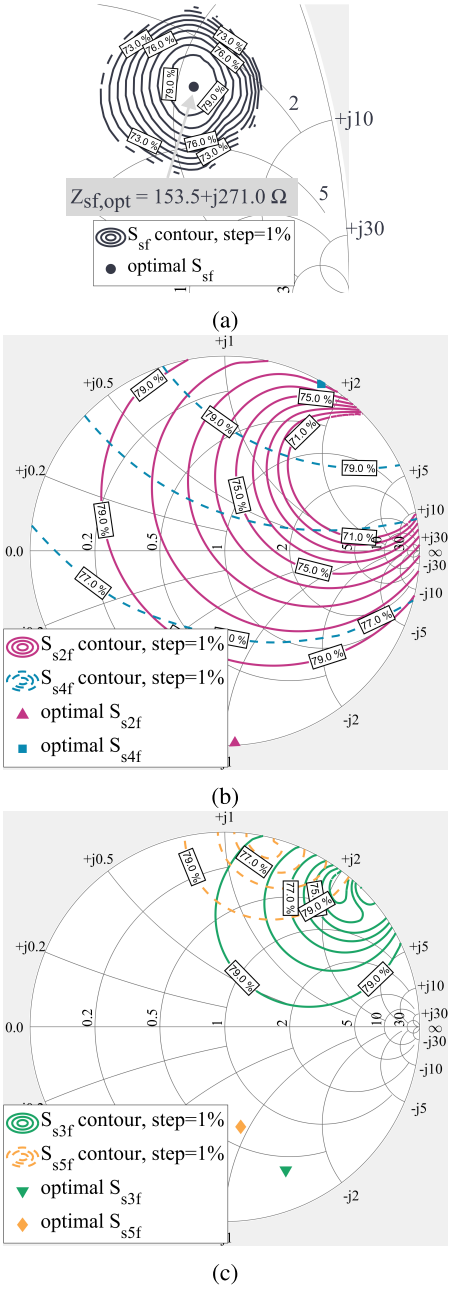

Fig. 6 Source-pull simulation results for the proposed single-series rectenna at an input power of 10.0 dBm, resulting in a dc output voltage of 2.84 V. (a) Contours at the fundamental frequency in the upper right of the Smith chart. (b) Contours at the second and fourth harmonics. (c) Copontours at the third and fifth harmonics.

source impedances for odd harmonics are less sensitive to the rf–dc conversion efficiency than are the fundamental and even harmonics. The rf–dc conversion efficiency becomes 79.0% or higher over a wide range in the lower left portion of the Smith chart for both the third and the fifth harmonics. The range of variation of the rf–dc conversion efficiency due to fluctuations of the source impedance is most significant for the fundamental wave, and this variation tends to decrease as the harmonic order increases. Lower-order harmonics substantially influence the rf–dc conversion efficiency because they possess higher energy [27]. In other words, when designing the receiving antenna, it is crucial to maintain the input impedance within the target range for the fundamental frequency.

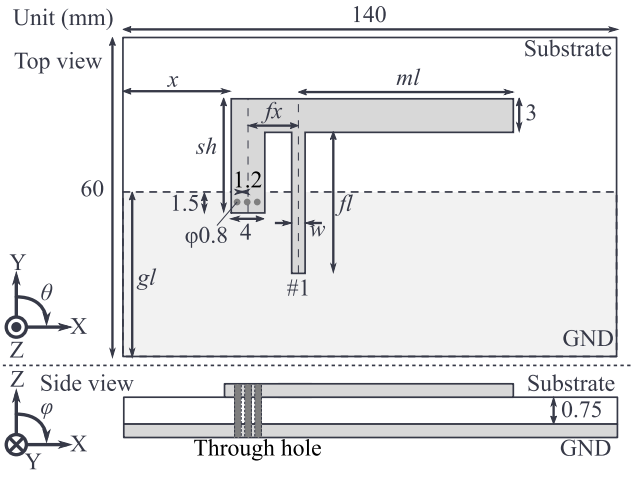

Fig. 7 Circuit diagram of the designed inverted-F antenna.

3.2 Antenna Design

Based on the results of the source-pull simulation shown in Fig. 6, we designed the receiving antenna. In a single-series rectenna, a short circuit on the anode side of the diode is required at dc to apply a reverse dc voltage to the diode. We adopted an inverted-F antenna with a short stub as the shape to satisfy this requirement. Figure 7 shows the designed inverted-F antenna, which we simulated using the T-solver of CST (Dassault Systemes) for antenna design. The substrate we used for the antenna was R5775-K. We connected a waveguide port toward the positive Y-axis at port #1 shown in Fig. 7 to analyze the antenna. We designed two types of receiving antennas using the inverted-F antenna geometry, as shown in Fig. 7: one for the proposed rectenna and another for the comparative rectenna. The dimensions indicated in Fig. 7 are the design parameters of the antennas. The proposed rectenna was designed so that the antenna input impedance at all harmonics falls within the target source impedance range for an rf–dc conversion efficiency of 79% or higher. The comparative rectenna was designed so only the antenna input impedance at the fundamental wave falls within the target range. To confirm that the harmonic control of the antenna impedance is effective in improving the rf–dc conversion efficiency in addition to the fundamental impedance matching, we compared the performance of the rectenna with harmonic control (proposed circuit) and the rectenna without harmonic control (comparative circuit).

Table 3 shows the adjusted design parameters of the inverted-F antenna with and without harmonic control. Figure 8 shows the frequency characteristics of the input impedance of the designed inverted-F antennas with and without harmonic control. The simulated and measured in-

Table 3 Adjusted parameters of the designed inverted-F antenna with and without harmonic control (HC).

	Parameter	Value (mm)	Parameter	Value (mm)
with HC	gl	35	fl	32.5
	ml	53.5	sh	18
	fx	3.5	w	0.3
	x	30.5		
without HC	gl	48	fl	41.5
	ml	62	sh	10
	fx	39	w	0.5
	x	18.5		

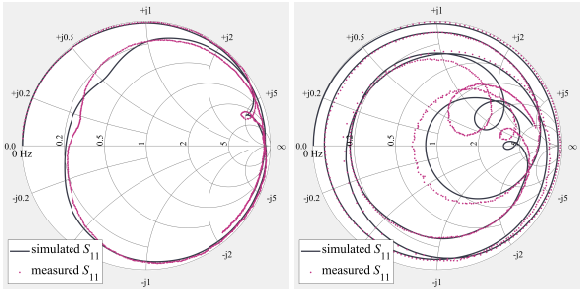

(a) (b)

Fig. 8 Simulated and measured input impedance of the inverted-F antenna with and without harmonic control from 0 Hz to 5 GHz. (a) The antenna with harmonic control. (b) The antenna without harmonic control.

put impedance of the designed antennas with and without harmonic control at each harmonic are shown in Fig. 9 along with the target impedance range. Specifically, Fig. 9 (a), Fig. 9 (b), and Fig. 9 (c) demonstrate that, in both the simulations and the measurements of the antenna with harmonic control, the input impedance at each harmonic falls within the target source-impedance range (i.e., an rf–dc conversion efficiency of 79.0% or higher). Furthermore, the input impedance of the antenna without harmonic control is within the target source impedance range only at the fundamental and fifth harmonic. For the second, third, and fourth harmonics, the input impedance of the antenna without harmonic control is outside the target source impedance range. From simulation results, the radiation efficiencies of the antennas with and without harmonic control at 920 MHz were 89.2% and 84.3%, and the maximum gains of the theta component on the XY plane were 1.64 dBi at $\theta = -7^\circ$ and 2.48 dBi at $\theta = -8^\circ$, respectively.

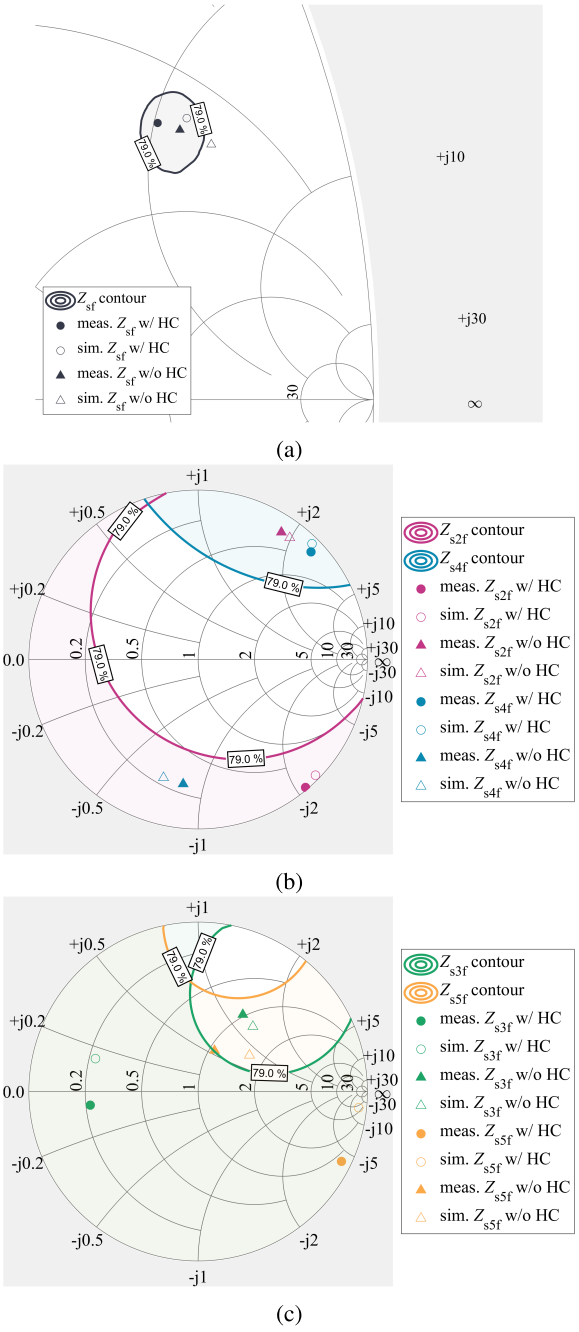

Fig. 9 Simulated and measured input impedances of the designed inverted-F antenna with and without harmonic control (HC) and the target source impedances at each harmonic. (a) Results at the fundamental frequency. (b) Results at the second and fourth harmonics. (c) Results at the third and fifth harmonics.

4. Rectenna Measurement

4.1 Input Power and Load Resisitance Characteristics of the Rectennas

Figure 10 shows the fabricated rectennas with and without harmonic control. We measured the input power and load resistance characteristics of the designed rectennas. Figure 11 and Fig. 12 show a photo and an outline of the measurement system of the rectenna in an anechoic chamber, respectively. In this measurement, we set the rectennas on the angle θ obtaining the peak output dc power. For estimating the actual input power to the rectifier circuit P_{in}, we measured the output power of the designed inverted-F antenna both with and without harmonic control using the measurement system shown in Fig. 12. We measured the received power of the antenna at the same angle as the rectenna measurement using the power sensor B before the rectenna measurement. We used a three stub tuner (MS-N-811, NIHON KOUSHUHA) and an SMA cable to perform impedance matching between

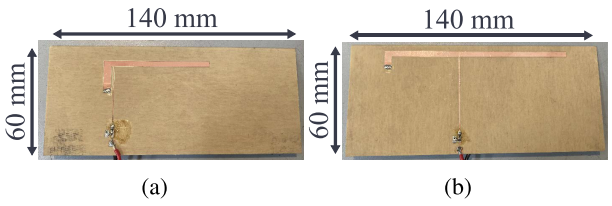

Fig. 10 Photos of the fabricated rectennas, (a) with harmonic control, (b) without harmonic control.

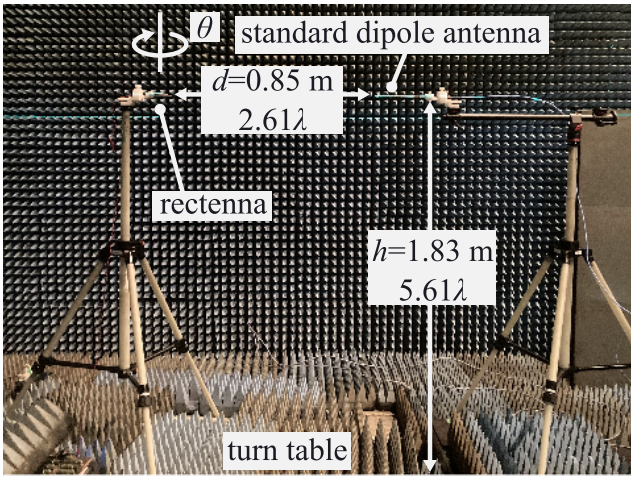

Fig. 11 Photo of the rectenna measurement system.

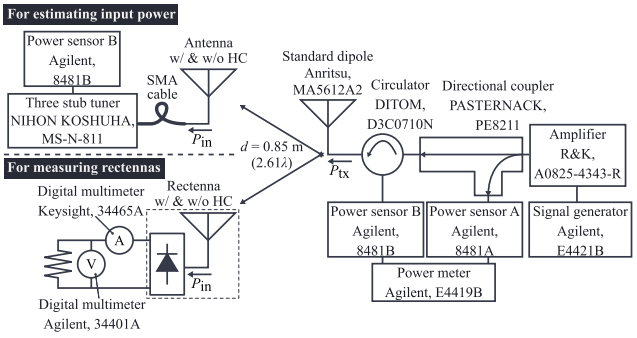

Fig. 12 Outline of the rectenna measurement system.

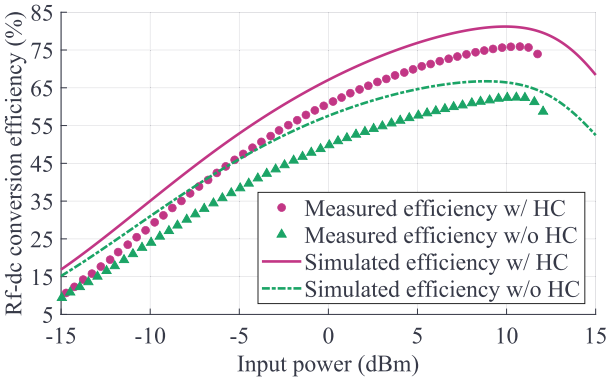

(a)

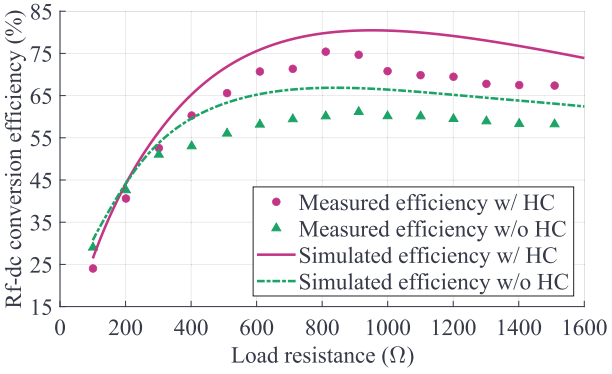

(b)

Fig. 13 Simulated and measured rf–dc conversion efficiency of the designed rectennas with and without harmonic control. (a) The rf–dc conversion efficiency vs. the input power at the load resistance of 1 kΩ. (b) The rf–dc conversion efficiency vs. the load resistance at the input power of 10.0 dBm.

Table 4 Performance comparison of the rectennas around 920 MHz band.

Ref.	Rectenna or Rectifier only	Rectifier type	Num. of diodes	Efficiency(%) at P_{in}(dBm)
[28]	Rectifier only	Single-shunt	1	66.0 at 9.0
[5]	Rectifier only	Single-shunt	1	80.4 at 13.4
[29]	Rectenna	Charge-pump	2	71.0 at 0.0
[30]	Rectenna	Charge-pump	2	71.0 at 15.0
[31]	Rectenna	Charge-pump	2	81.0 at 11.0
[32]	Rectenna	Charge-pump	2	83.0 at -4.0
This work	Rectenna	Single-series	1	75.9 at 10.8

the designed inverted-F antenna and the system reference impedance of 50 Ω. We measured the insertion loss of the three stub tuner and the SMA cable used in the received power measurement as shown in Fig. 12. Then, the actual input power to the rectifier circuit P_{in} was determined by deducting the insertion loss of the three-stub tuner and cable from the received power.

Figure 13 shows the simulated and measured rf–dc conversion efficiency of the designed rectennas. Figure 13 shows that the maximum measured rf–dc conversion efficiency of the rectenna with and without reached 75.9% at an input power of 10.8 dBm and load resistance of 1 kΩ and 62.4% at an input power of 10.6 dBm and load resistance of 1 kΩ, respectively. Both simulated and measured results show that the proposed rectenna with harmonic control of the antenna impedance has higher rf-dc conversion efficiency than the comparative rectenna without harmonic control. Thus, these comparative results confirm that the harmonic control of the antenna impedance effectively enhances the rf–dc conversion efficiency. Table 4 compares the performance of rectennas operating in the 920 MHz band, demonstrating that the proposed rectenna achieves superior efficiency with just a single diode compared to previous studies.

4.2 Angular Characteristics of the Rectenna

The radiation patterns of the proposed rectenna were evaluated on the XY and YZ planes utilizing the far-field measurement system in an anechoic chamber. Additionally, the

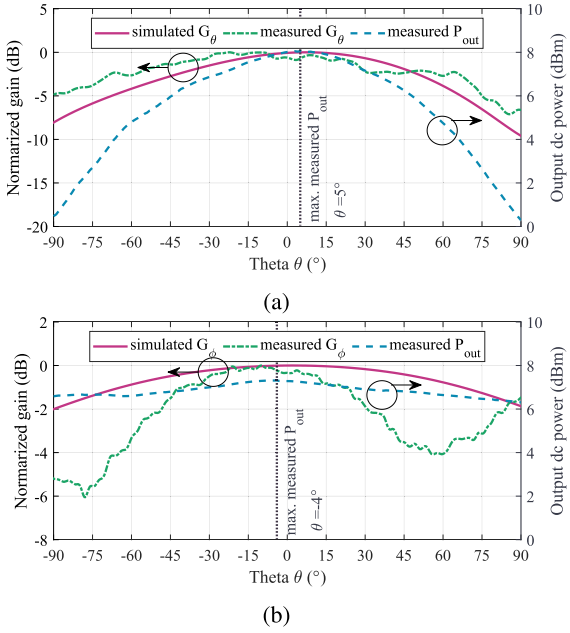

Fig. 14 Simulattion and measurement results of the normalized gain of the designed antenna and the angular characteristics of the output dc power of the designed rectenna. (a) Results on the XY plane. (b) Results on the YZ plane.

angular characteristics of the output dc power of the proposed rectenna were measured in another anechoic chamber. During the angular characteristics measurements, the transmission power P_{tx} was set to 35 dBm, and a load resistance of 1 kΩ was employed. The turntable shown in Fig. 11 facilitated the angular measurements. Figure 14 shows both simulated and experimental results related to the radiation patterns of the designed inverted-F antenna and the angular characteristics of the proposed rectenna. It is noted that the radiation pattern results have been normalized to their peak values. The peak output dc power of the rectenna with harmonic control was higher in the XY plane than in the YZ plane. The peak output dc power and angle of the rectenna with harmonic control were 8.05 dBm and 5° on the XY plane, respectively.

5. Conclusion

This study demonstrated that a novel single-diode rectenna can improve the rf–dc conversion efficiency through harmonic control of the antenna impedance. We employed source-pull simulations encompassing the fundamental frequency and the harmonics to achieve a highly efficient rectenna. Based on the source-pull simulation results, we designed the inverted-F antenna. Subsequently, we performed experimental measurements using the fabricated rectennas. Our findings indicate that the maximum rf–dc conversion efficiency for the designed rectenna reached 75.9% at an input power of 10.8 dBm and a load resistance of 1 kΩ. These measurements and comparisons with the comparative rectenna and previous studies underscore the achievement of full-wave rectification and high efficiency in the proposed single-series rectenna, where harmonic control is executed at the receiving antenna.

Acknowledgments

The authors are grateful to Professor Ryo Ishikawa from The University of Electro-Communications for teaching the fundamentals of source/load-pull techniques. This work was supported by JSPS KAKENHI Grant Number 22KJ1853. Part of this research was carried out by use of Microwave Energy Transmission Laboratory (METLAB) as collaborative inter-university research facility in Research Institute for Sustainable Humanosphere (RISH), Kyoto University.

References

[1] W.C. Brown, "The history of the development of the rectenna," NASA. Johnson Space Center Solar Power Satellite Microwave Transmission and Reception, 1980.
[2] N. Shinohara, "Rectennas for microwave power transmission," IEICE Electron. Express, vol.10, no.21, pp.20132009–20132009, 2013.
[3] C. Wang, B. Yang, and N. Shinohara, "Study and design of a 2.45-ghz rectifier achieving 91% efficiency at 5-w input power," IEEE Microw. Compon. Lett., vol.31, no.1, pp.76–79, 2021.
[4] K. Kawai, N. Shinohara, and T. Mitani, "Novel structure of single-shunt rectifier circuit with impedance matching at output filter," IEICE Trans. Electron., vol.E106-C, no.2, pp.50–58, 2023.
[5] J. Guo, H. Zhang, and X. Zhu, "Theoretical analysis of rf-dc conversion efficiency for class-f rectifiers," IEEE Trans. Microw. Theory Techn., vol.62, no.4, pp.977–985, 2014.
[6] H. Mei, X. Yang, B. Han, and G. Tan, "High-efficiency microstrip rectenna for microwave power transmission at ka band with low cost," IET Microwaves, Antennas & Propagation, vol.10, no.15, pp.1648–1655, 2016.
[7] K. Hatano, N. Shinohara, T. Mitani, K. Nishikawa, T. Seki, and K. Hiraga, "Development of class-f load rectennas," 2011 IEEE Trans. Microw. Theory Techn.-S International Microwave Workshop Series on Innovative Wireless Power Transmission: Technologies, Systems, and Applications, pp.251–254, 2011.
[8] J.O. McSpadden, Lu Fan, and Kai Chang, "Design and experiments of a high-conversion-efficiency 5.8-ghz rectenna," IEEE Trans. Microw. Theory Techn., vol.46, no.12, pp.2053–2060, 1998.
[9] N. Sakai, K. Noguchi, and K. Itoh, "A 5.8-ghz band highly efficient 1-w rectenna with short-stub-connected high-impedance dipole antenna," IEEE Trans. Microw. Theory Techn., vol.69, no.7, pp.3558–3566, 2021.
[10] S. Gao, P. Butterworth, S. Ooi, and A. Sambell, "High-efficiency power amplifier design including input harmonic termination," IEEE Microw. Compon. Lett., vol.16, no.2, pp.81–83, 2006.
[11] P. Colantonio, F. Giannini, E. Limiti, and V. Teppati, "An approach to harmonic load- and source-pull measurements for high-efficiency pa design," IEEE Trans. Microw. Theory Techn., vol.52, no.1, pp.191–198, 2004.
[12] J. Enomoto, R. Ishikawa, and K. Honjo, "Second harmonic control technique for bandwidth enhancement of gan hemt amplifier with harmonic reactive terminations," IEEE Trans. Microw. Theory Techn., vol.65, no.12, pp.4947–4952, 2017.
[13] M.N. Ruiz and J.A. García, "An e-phemt self-biased and self-synchronous class e rectifier," 2014 IEEE Trans. Microw. Theory Techn.-S International Microwave Symposium (IMS2014), pp.1–4, 2014.
[14] S. Abbasian and T. Johnson, "High efficiency and high power gan hemt inverse class-f synchronous rectifier for wireless power applications," 2015 European Microwave Conference (EuMC), pp.299–302,

2015.
[15] I. Ramos and Z. Popović, "A compact 2.45 ghz, low power wireless energy harvester with a reflector-backed folded dipole rectenna," 2015 IEEE Wireless Power Transfer Conference (WPTC), pp.1–3, 2015.
[16] I. Ramos, M.N. Ruiz, J.A. García, D. Maksimović, and Z. Popović, "A planar 75% efficient gan 1.2-ghz dc-dc converter with self-synchronous rectifier," 2015 IEEE Trans. Microw. Theory Techn.-S International Microwave Symposium, pp.1–4, 2015.
[17] M.A. Hoque, S.N. Ali, M.A. Mokri, S. Gopal, M. Chahardori, and D. Heo, "A highly efficient dual-band harmonic-tuned gan rf synchronous rectifier with integrated coupler and phase shifter," 2019 IEEE Trans. Microw. Theory Techn.-S International Microwave Symposium (IMS), pp.1320–1323, 2019.
[18] E. Falkenstein, M. Roberg, and Z. Popovic, "Low-power wireless power delivery," IEEE Trans. Microw. Theory Techn., vol.60, no.7, pp.2277–2286, 2012.
[19] M. Roberg, T. Reveyrand, I. Ramos, E.A. Falkenstein, and Z. Popovic, "High-efficiency harmonically terminated diode and transistor rectifiers," IEEE Trans. Microw. Theory Techn., vol.60, no.12, pp.4043–4052, 2012.
[20] D. Wang, X.A. Nghiem, and R. Negra, "Design of a 57 % bandwidth microwave rectifier for powering application," 2014 IEEE Wireless Power Transfer Conference, pp.68–71, 2014.
[21] A. Alt, R. Quaglia, P. Chen, S. Alsahali, P.J. Tasker, and J. Lees, "Analysis of highly efficient self-synchronous class-f microwave rectifiers using waveform engineering," 2018 48th European Microwave Conference (EuMC), pp.773–776, 2018.
[22] C.-H. Tsai, I.-N. Liao, C. Pakasiri, H.-C. Pan, and Y.-J. Wang, "A wideband 20 mw uhf rectifier in cmos," IEEE Microw. Compon. Lett., vol.25, no.6, pp.388–390, 2015.
[23] M. Machida, R. Ishikawa, Y. Takayama, and K. Honjo, "Ghz-band high-efficiency rectifier design based on mhz-band multi - harmonic active source-pull technique," 2018 IEEE/MTT-S International Microwave Symposium - IMS, pp.1134–1137, 2018.
[24] F. Zhao, D. Inserra, G. Wen, J. Li, and Y. Huang, "A high-efficiency inverse class-f microwave rectifier for wireless power transmission," IEEE Microw. Compon. Lett., vol.29, no.11, pp.725–728, 2019.
[25] D.M. Nguyen, N.D. Au, and C. Seo, "A microwave power transmission system using sequential phase ring antenna and inverted class f rectenna," IEEE Access, vol.9, pp.134163–134173, 2021.
[26] T. Ohira, "Power efficiency and optimum load formulas on rf rectifiers featuring flow-angle equations," IEICE Electron. Express, vol.10, no.11, pp.20130230–20130230, 2013.
[27] S.D. Joseph, Y. Huang, S.S.H. Hsu, A. Alieldin, and C. Song, "Second harmonic exploitation for high-efficiency wireless power transfer using duplexing rectenna," IEEE Trans. Microw. Theory Techn., vol.69, no.1, pp.482–494, 2021.
[28] X. Wang, O. Abdelatty, and A. Mortazawi, "Design of a wide dynamic range rectifier array with an adaptive power distribution technique," 2016 46th European Microwave Conference (EuMC), pp.922–925, 2016.
[29] G. Moloudian, J.L. Buckley, and B. O'Flynn, "A novel rectenna with class-f harmonic structure for wireless power transfer," IEEE Trans. Circuits Syst. II, Exp. Briefs, vol.71, no.2, pp.617–621, 2024.
[30] J. Shen, W. Zhang, C. Wu, X. Wu, E. Fang, and X. Liu, "A compact duplexing rectenna with wireless power transfer and harmonic feedback capabilities," IEEE Antennas Wireless Propag. Lett., vol.22, no.7, pp.1751–1755, 2023.
[31] M. Wagih, A.S. Weddell, and S. Beeby, "Dispenser printed flexible rectenna for dual-ism band high-efficiency supercapacitor charging," 2021 IEEE Wireless Power Transfer Conference (WPTC), pp.1–4, 2021.
[32] M. Wagih, A.S. Weddell, and S. Beeby, "High-efficiency sub-1 ghz flexible compact rectenna based on parametric antenna-rectifier co-design," 2020 IEEE/MTT-S International Microwave Symposium (IMS), pp.1066–1069, 2020.

Katsumi Kawai received the B.E. degree in electrical and electronic engineering from Kobe City College of Technology, Japan, in 2019. He received the M.E. degree in electrical engineering from Kyoto University, Japan, in 2021. He is currently pursuing the Ph.D degree in electrical engineering. His current reserch interests include rectenna and wireless power transfer system design.

Naoki Shinohara received the B.E. degree in electronic engineering, the M.E. and Ph.D (Eng.) degrees in electrical engineering from Kyoto University, Japan, in 1991, 1993 and 1996, respectively. He was a research associate in Kyoto University from 1996. From 2010, he has been a professor in Kyoto University. He has been engaged in research on Solar Power Station/Satellite and Microwave Power Transmission system. He was IEEE MTT-S Distinguish Microwave Lecturer (2016–18), and is IEEE AdCom member (2022–2024), IEEE MTT-S Technical Committee 25 (Wireless Power Transfer and Conversion) former chair and member, IEEE MTT-S MGA (Member Geographic Activities) Region 10 regional coordinator, IEEE WPT Initiative Member, IEEE MTT-S Kansai Chapter TPC member, IEEE Wireless Power Transfer Conference founder and Steering committee member, URSI commission D chair, international journal of Wireless Power Transfer (Hindawi) executive editor, the first chair and technical committee member on IEICE Wireless Power Transfer, Japan Society of Electromagnetic Wave Energy Applications adviser, Space Solar Power Systems Society vice chair, Wireless Power Transfer Consortium for Practical Applications (WiPoT) chair, and Wireless Power Management Consortium (WPMc) chair. His books are "Wireless Power Transfer via Radiowaves" (ISTE Ltd.) and John Wiley & Sons, Inc., "Recent Wireless Power Transfer Technologies Via Radio Waves (ed.)" (River Publishers), and "Wireless Power Transfer: Theory, Technology, and Applications (ed.)" (IET), and some Japanese text books of WPT.

Tomohiko Mitani received the B.E. degree in electrical and electronic engineering, the M.E. degree in informatics, and the Ph.D. in electrical engineering from Kyoto University, Kyoto, Japan, in 1999, 2001, and 2006, respectively. He was an Assistant Professor with the Radio Science Center for Space and Atmosphere, Kyoto University, in 2003. He has been an Associate Professor with the Research Institute for Sustainable Humanosphere, Kyoto University, since 2012. His current research interests include microwave heating application and microwave power transfer. He has been a board member of Japan Society of Electromagnetic Wave Energy Applications (JEMEA) since 2014. He was a treasurer of IEEE MTT-S Kansai Chapter from 2014 to 2017, and from 2019 to 2021. He has been a technical committee chair of IEEE MTT-S Kansai Chapter since 2022.